

# Coding of the Reach Vector in Parietal Area 5d

Lindsay R. Bremner<sup>1,\*</sup> and Richard A. Andersen<sup>1</sup>

<sup>1</sup>Division of Biology, California Institute of Technology, Pasadena, CA 91125, USA

\*Correspondence: [lindsay@vis.caltech.edu](mailto:lindsay@vis.caltech.edu)

<http://dx.doi.org/10.1016/j.neuron.2012.03.041>

## SUMMARY

Competing models of sensorimotor computation predict different topological constraints in the brain. Some models propose population coding of particular reference frames in anatomically distinct nodes, whereas others require no such dedicated subpopulations and instead predict that regions will simultaneously code in multiple, intermediate, reference frames. Current empirical evidence is conflicting, partly due to difficulties involved in identifying underlying reference frames. Here, we independently varied the locations of hand, gaze, and target over many positions while recording from the dorsal aspect of parietal area 5. We find that the target is represented in a predominantly hand-centered reference frame here, contrasting with the relative code seen in dorsal premotor cortex and the mostly gaze-centered reference frame in the parietal reach region. This supports the hypothesis that different nodes of the sensorimotor circuit contain distinct and systematic representations, and this constrains the types of computational model that are neurobiologically relevant.

## INTRODUCTION

Imagine sitting in a meeting and reaching out to pick up a doughnut. We are easily able to reach to it accurately, even if we are looking at the speaker rather than at the doughnut directly, yet this seemingly simple behavior requires the brain to solve a nontrivial computational problem. Information about the location of the doughnut, or visual target, is initially represented in the brain in retinotopic coordinates, a gaze- or eye-centered frame of reference, but the reach itself can be thought of as a vector that starts at the current location of the hand and ends at the target, and has little to do with the direction of gaze. To make an accurate reach, the information about target location must be transformed from the initial gaze-centered reference frame to a hand or body-centered reference frame, and ultimately into a series of motor commands sent to the muscles (Andersen and Buneo, 2002; Kalaska et al., 1997).

There is broad agreement that reciprocally connected circuits between posterior parietal and frontal cortex are involved in the sensorimotor transformation (Andersen and Cui, 2009; Caminiti et al., 1998), but the nature of the underlying computation

is controversial. Traditionally, the transformation was thought to occur systematically, either in hierarchical stages—from gaze to head to body to shoulder, etc. (Flanders et al., 1992)—or via a common, gaze-centered, reference frame that is gain modulated by postural eye and hand position signals (Andersen et al., 1998; Batista et al., 1999; Buneo et al., 2002; Cohen and Andersen, 2002; Pesaran et al., 2006; Zipser and Andersen, 1988). In the hierarchical model, one would expect to find many different representations of space in distinct neuronal populations. In the common reference frame model one would likewise expect to find dedicated populations of neurons but for gaze-centered reference frames (combined with the appropriate postural gain signals) and downstream output reference frames.

This framework has been challenged by theoretical studies showing that such systematic and modular reference frames may not be necessary (Blohm et al., 2009; McGuire and Sabes, 2009; Pouget et al., 2002; Pouget and Snyder, 2000). Instead, single areas could encode large numbers of signals simultaneously, forming a set of basis functions from which multiple outputs can be flexibly read. This model predicts that the brain does not have sub-regions coding in particular reference frames but instead has areas with large degrees of mixed and intermediate reference frames. The theories therefore make quite distinct topological predictions, with implications beyond sensorimotor transformations to underlying issues about the general structure and processing of information in the brain.

A number of previous experiments have demonstrated a predominance of gaze-centered coding of reaches in the parietal reach region (PRR) (Andersen et al., 1998; Batista et al., 1999; Buneo et al., 2002; Cohen and Andersen, 2002; Pesaran et al., 2006). Furthermore, negatively correlated hand and eye gain fields have been reported within individual cells in PRR (Chang et al., 2009), indicative of systematic organization of information. In contrast, there have recently been many reports of intermediate and mixed reference frames in both posterior parietal and frontal cortex (Avillac et al., 2005; Batista et al., 2007; Battaglia-Mayer et al., 2003; Chang and Snyder, 2010; Cohen and Andersen, 2000; McGuire and Sabes, 2011; Mullette-Gillman et al., 2005, 2009; Stricanne et al., 1996).

One explanation for the proliferation of conflicting results is that it can be difficult in practice to distinguish an underlying reference frame from scaling, gain field effects that are also commonly present (Andersen et al., 1985, 1990; Andersen and Mountcastle, 1983; Bremner et al., 1999; Galletti et al., 1995; Nakamura et al., 1999), but this distinction is critical to avoid miscategorization. For example, cells in dorsal premotor cortex (PMd) can appear heterogeneous or with no clear reference frame (Batista et al., 2007). However, when recorded in a task

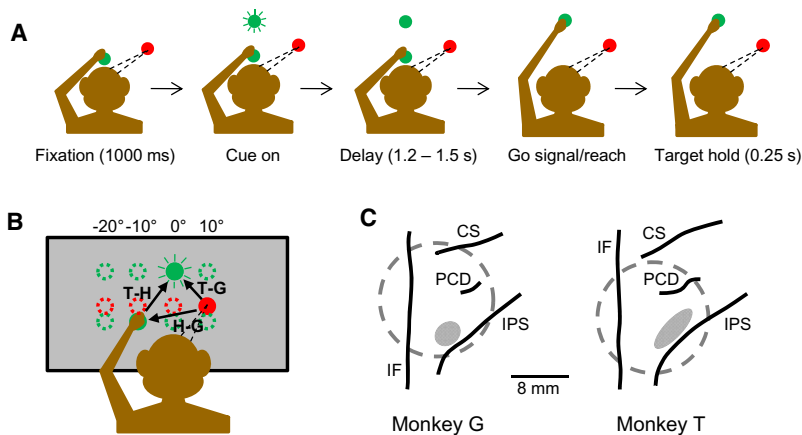


**Figure 1. The Experimental Design and Recording Sites**

(A) The timeline of the delayed reaching task for a single trial (see [Experimental Procedures](#) for details).

(B) The geometry of the reference frame task. The monkey was trained to reach from one of four possible starting hand positions to one of four targets (green circles), while maintaining gaze fixation at one of four locations (red circles). Fixation positions and targets were 10 degrees (approximately 5 cm) apart horizontally in screen-centered coordinates.

(C) Location of the recording zones for each monkey estimated from structural magnetic resonance images. CS, central sulcus; IPS, intraparietal sulcus; PCD, post-central dimple; IF, interhemispheric fissure; dotted gray circle, recording chamber; shaded ellipse, recording zone.

in which multiplicative gain could be teased apart from true shifts of the tuning curve, neurons in this region did in fact show order: they encoded the locations of the hand, gaze, and target relative to each other in extrinsic space, referred to as a full relative code (Pesaran et al., 2006).

Many studies have been conducted on the reference frames in PRR, lateral intraparietal cortex (LIP) and PMd, but relatively few have looked at the neighboring dorsal area 5 (area 5d). Body-centered (Lacquaniti et al., 1995), intermediate (Buneo et al., 2002), and heterogeneous (McGuire and Sabes, 2011) reference frames have all been reported in area 5d, but none of these previous studies adequately tested enough variables. Here, we independently varied the positions of the gaze, hand, and target over a range of locations while recording from cells in macaque area 5d and identified a predominantly hand-centered representation of the reach target. Given the different theoretical predictions described above, it was important to assess the degree of heterogeneity among cells in area 5d and whether it has a population code distinct from other nodes of the reaching circuit.

## RESULTS

For an understanding of the potential neural computations involved in coordinate transformations, it is essential to be able to distinguish the underlying reference frame of a cell from gain field effects that can also influence its firing rate (Andersen and Mountcastle, 1983). This can be difficult to implement in practice because a large number of trial types is necessary to vary the experimental parameters independently across a broad enough range of space.

We used the delayed-reach experimental design and analysis of Pesaran et al. with four target locations (T), four starting hand positions (H), and four gaze-fixation points (G), for a total of 64 different trial types (Figure 1B) (Pesaran et al., 2006). This design allowed us to fully characterize whether cell firing rates encoded the target position relative to gaze direction (T-G), the target position relative to the hand (T-H), hand position relative to gaze direction (H-G), or a combination of these vectors. It also enabled us to make direct comparisons between our results from area 5d and earlier data from PRR and PMd (Pesaran et al., 2006, 2010).

The data were aligned at movement onset (0 ms) and the delay period was defined as  $-500$  to  $-100$  ms. For each neuron, mean firing rates during the delay period were converted into twelve firing rate response matrices, four for each of the three possible combinations of variables (TH, TG, HG; see Figure S1 available online). For example, a single 4-by-4 target-hand (TH) matrix represents the firing rates for all 16 different arrangements of target location and starting hand position, but with gaze position constant at, say,  $-20$  degrees in all trials. The other three TH matrices have the same target and hand structure, but are composed of trials in which gaze was located at  $-10$ ,  $0$ , or  $10$  degrees, respectively. Each element within a matrix therefore represents the mean firing rate for a single trial type. The TG matrices, in which H was held constant, and the HG matrices, in which T was held constant, were formed similarly. The main analysis was conducted on the subset of matrices in which the third variable was held constant at the response field peak (e.g., gaze at  $-10$  degrees for a TH matrix). This results in a set of three matrices per neuron, one for each variable pair (see Figure 3B and Figure S1).

Figures 2A and 2B (left panels) illustrate how a matrix would appear for an idealized cell with a purely gain field relationship between a given pair of variables (T and H in this example). The peak of the tuning curve for T remains located at the same extrinsic position ( $-10$  degrees) for all values of H, with the effect of H being to scale the magnitude of the response. In other words, changes in H and T produce multiplicatively separable changes in the response of the cell. Figure 2C shows the quite distinct “diagonal” pattern for an idealized cell that codes the extrinsic reach vector T-H: the peak of the tuning curve for T shifts as H is varied. The influence of the two variables cannot be separated from each other in this hand-centered reference frame for target position. Such a vector relationship need not involve full shifts (Figure 2D). Furthermore, cells may simultaneously represent both a vector and a postural gain field (Figure 2E). A population of cells of this type could contain a distributed code for the location of the target in head/body-centered space (Andersen et al., 1990; Zipser and Andersen, 1988).

We used singular value decomposition (SVD) to determine whether each variable-pair matrix was separable or inseparable, and hence whether the defining relationship between a pair of

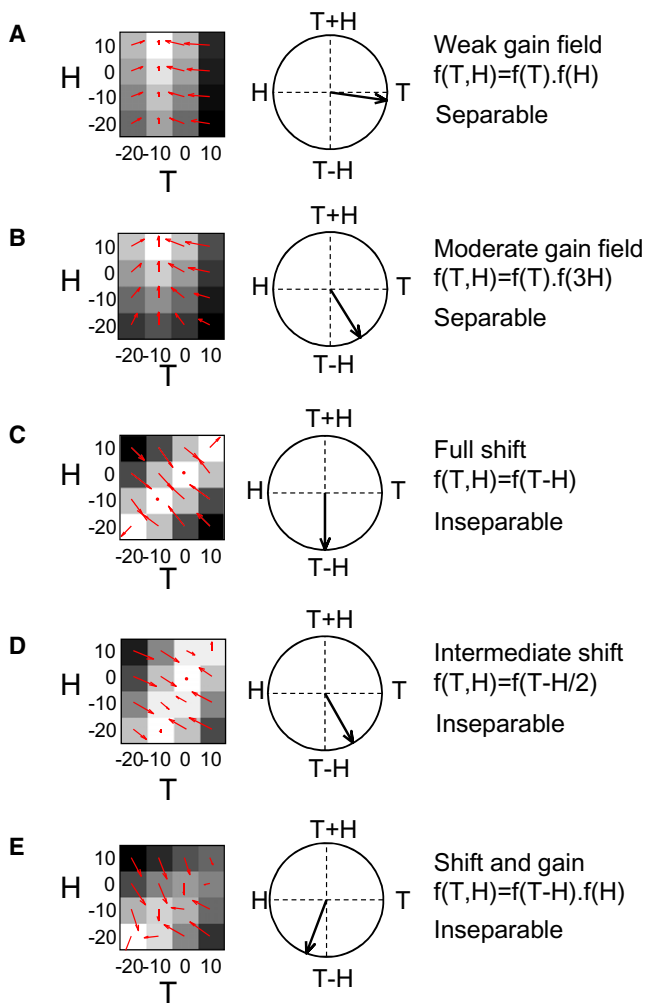


**Figure 2. Gain Field and Vector Relationships Illustrated in Simulated Cells**

(A) A cell with a weak gain field of hand (H) on target (T).  
 (B) A cell with a moderate gain field of H on T.  
 (C) A cell with a vector relationship between H and T (full shift).  
 (D) A cell with a vector relationship between H and T (intermediate shift).  
 (E) A cell with a vector relationship between H and T plus a superimposed H gain field.

Left panels show idealized matrix responses for a pair of variables (illustrated here with H and T). White represents a high firing rate and black represents a low firing rate. Small red arrows denote the gradient of each matrix response field. Center panels show the overall response field orientation calculated from the red gradient arrows. The response field orientation indicates the relative influence of each variable on the firing rate of the cell. Right panels list how each simulated cell was modeled and whether each type of relationship is categorized as separable or inseparable in the SVD analysis.

variables for a cell was better described as a gain field or as a vector (Peña and Konishi, 2001; Pesaran et al., 2006, 2010). In conjunction with this analysis, we also used gradient analysis to assess whether a cell was significantly tuned for a particular variable pair and, if so, which of the two variables exerted the most influence on the firing rate of the cell (Figure 2, middle panels; Experimental Procedures).

### Heterogeneity in Individual Cells

We recorded 128 cells from parietal area 5d in two animals (79 in monkey G, 49 in monkey T). Both monkeys were well trained in the task before recordings began and had typical success rates of 78%–84% trials correct for monkey G and 70%–78% trials correct for monkey T. Reaction times were comparable with means (and standard deviations) of 314 (132) ms (monkey G) and 289 (120) ms (monkey T). Results from both monkeys were qualitatively similar, so data were pooled across animals in all analyses.

Figure 3 shows an example of a cell that codes target location in hand-centered coordinates. The response profile in the poststimulus time histogram (Figure 3A) is typical of neurons recorded in area 5d: The cell showed little response to the visual stimulation produced by cue onset but increased its firing as the delay period progressed, with peak firing occurring around the time of movement initiation. The delay-period activity used in the main analysis is denoted by the shaded region.

The mean delay-period activity for this cell across different trial conditions is presented in Figure 3B. The TH matrix for this cell is inseparable with a gradient resultant of  $-83$  degrees, indicating that the response field for reach targets shifted almost completely with the initial position of the hand. Moreover, the TG and HG matrices were both separable and encoded T and H, respectively (11 degrees and 5 degrees), as would be expected for a cell encoding the relative position of the hand and the target.

From the population of recorded cells, 71/128 (55%) were significantly tuned to at least one of the variable pairs. Of these, we identified 19 cells (27%) which coded either the target relative to the hand (T-H, 11 cells), the target relative to gaze (T-G, 7 cells) or the hand relative to gaze (H-G, just 1 cell) in a similarly complete fashion across all three response matrices (see Experimental Procedures and Table 1). This heterogeneity at the level of individual cells is in agreement with other recent reports from closely related parietal regions (Chang and Snyder, 2010; McGuire and Sabes, 2011). The remaining 73% of cells had gradient resultants that reached significance in only a subset of the variable-pair matrices, showed only gain fields, or coded for more than one vector.

### Hand-Centered Population Coding

Despite the heterogeneity in individual cells, a clear pattern of coding emerged when we looked at the population as a whole. This difference between the population and individual cell results is likely due to the exclusion of 73% of tuned cells from the stringent categorization of individual cells described above, even though these cells were significantly tuned to at least one variable pair. The population analysis included these cells, and so gives a more comprehensive indication of the role of the area.

Hand-centered coding for target location was dominant at the population level: 53/128 (41%) cells were significantly tuned to the TH variable pair. The majority of these cells were inseparable (35/53; 66%), and the distribution of resultant angles was strongly nonuniform ( $p < 0.0001$ ; Kuiper test) and unimodally distributed ( $p < 0.0001$ ; Rayleigh test) with a mean

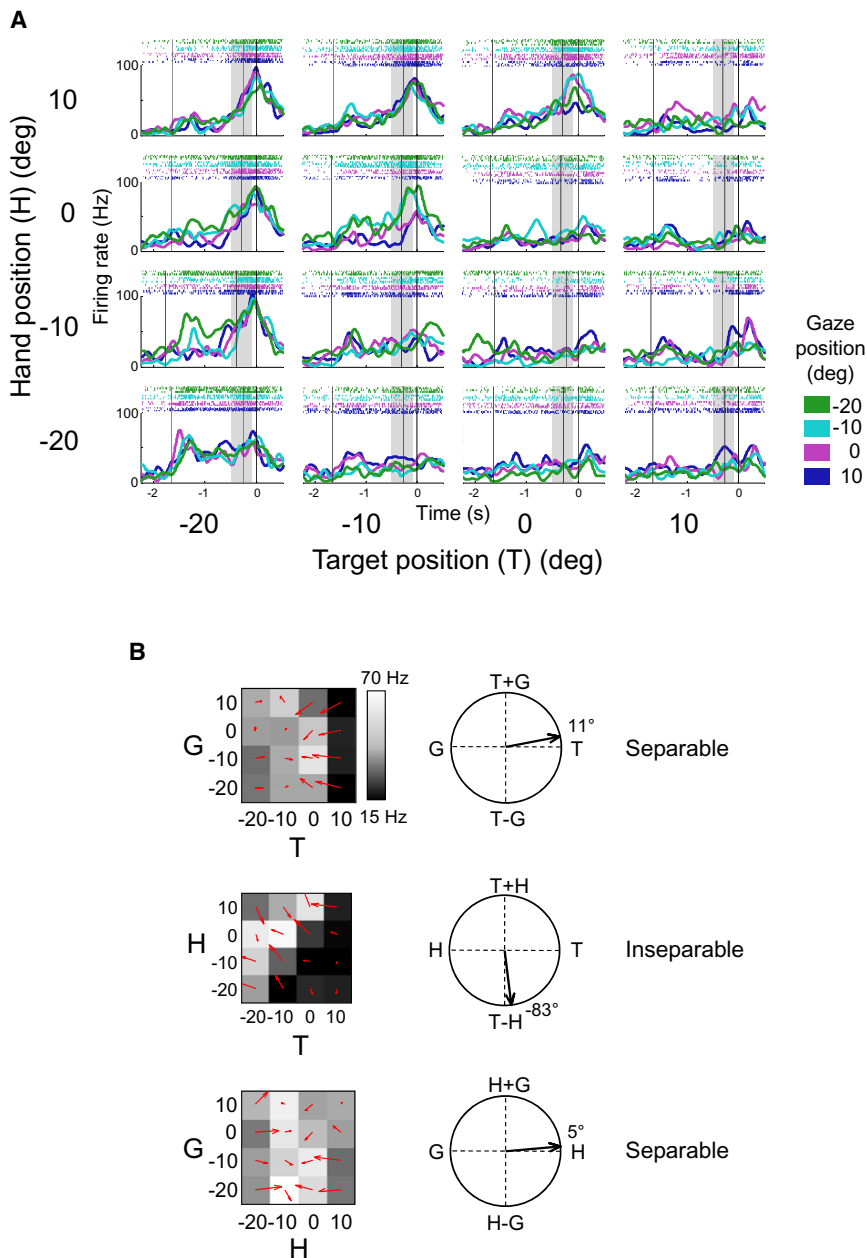


**Figure 3. Example Area 5d Cell with Hand-Centered Reference Frame**

(A) Peristimulus time histograms and raster plots for the 64 conditions. Each of the 16 subplots shows the response of the neuron to a particular combination of target position (T) and hand position (H) at the four different gaze locations (G). For example, the top left plot shows trials in which the target was located at  $-20$  degrees, the hand started at  $10$  degrees, and the gaze was fixed at  $-20$  degrees (green line),  $-10$  degrees (cyan line),  $0$  degrees (purple line), or  $10$  degrees (dark blue line). Trials are aligned to movement onset (solid vertical line in each subplot), with the first and second dashed lines indicating mean times for cue onset and the go signal, respectively. The shaded bar indicates the late delay period used in the analysis. For this cell, gaze position only weakly influenced the firing of the cell so the colored traces largely overlap in each subplot.

(B) Matrices and response field orientations for the cell shown in (A). Top: the target-gaze matrix (hand at  $10$  degrees, formed from the top row of subplots in (A)). Middle: the target-hand matrix (gaze at  $-10$  degrees, formed from all the cyan traces in (A)). Bottom: the gaze-hand matrix (target at  $-20$  degrees, formed from the left-most column of subplots in (A)).

Figure S1 shows the full complement of 12 matrices for this cell.

distribution of resultant angles was not significantly different from uniform (Kuiper test, Figure 4, bottom panel). This indicates that although hand position and/or gaze direction influenced the firing rate of these cells, they were not encoding the hand-gaze vector.

The greater strength of population tuning for the T-H vector versus T-G or H-G is reflected in the proportion of cells with a tuned and inseparable response for that vector. Fifty-six cells had at least one matrix that was both significantly tuned and inseparable. Of these, 35 cells (63%) coded for T-H, compared with 19 cells (34%) for T-G and 18 cells (32%) for H-G. As shown in Figure 5A, the majority of cells coded for only one of the three vectors (39% for T-H, 18% for T-G, and 14% for H-G), but a small number of cells jointly encoded T-H and T-G (6/56; 11%), T-H and H-G (7/56; 13%), or T-G and H-G (3/56; 5%) in their individual responses. We did not find any cells that were tuned and inseparable for all three matrices. This is in contrast to PMd, where single cells tend to code two or all three vectors (Pesaran et al., 2006) (Figure 5B).

It is possible that other patterns of tuning may exist away from the response field peaks. However, when we conducted a similar analysis across all hand, gaze, and target positions, the results were very consistent, with hand-centered tuning dominating the responses (Figure S2).

response field orientation of  $-73$  degrees (Figure 4, middle panel).

Gaze-centered coding was weakly but significantly represented in the population. Fewer cells were significantly tuned to the TG variable pair (35/128; 27%) and of those that were tuned slightly more than half (19/35; 54%) were classed as inseparable. The mean response field orientation was  $-37$  degrees, with a nonuniform and unimodal distribution (Kuiper test  $p < 0.0001$ ; Rayleigh test  $p < 0.0001$ ; Figure 4, top panel). Strikingly, we did not see evidence for coding of the position of the hand relative to gaze location at the population level in area 5d. Of the 36/128 cells (28%) that were significantly tuned to the HG variable pair, 18/36 (50%) were inseparable, but the

**Table 1. Criteria for Categorizing Individual Cells**

Parameter	Significantly Tuned?	Response Field		
		Orientation (degrees)	Separability	
Hand centered (11 cells satisfy 8/9 criteria)	TH	Yes (53)	-90 (86)	Inseparable (103)
	TG	Yes (35)	0 (62)	Separable (26)
	HG	Yes (36)	0 (49)	Separable (30)
Gaze centered (7 cells satisfy 8/9 criteria)	TH	Yes (53)	0 (43)	Separable (25)
	TG	Yes (35)	-90 (59)	Inseparable (102)
	HG	Yes (36)	-180 (31)	Separable (30)
Hand gaze (1 cell satisfies 8/9 criteria)	TH	Yes (53)	-180 (27)	Separable (25)
	TG	Yes (35)	-180 (21)	Separable (26)
	HG	Yes (36)	-90 (62)	Inseparable (98)

The numbers of cells within each category are shown in parentheses (total n = 128).

**Population Model Fitting**

Model fitting is a complementary approach that we used to verify the findings from the SVD/gradient analysis. For each cell, we fit the delay-period firing rates from all 64 trial types to the following parametric model (Chang et al., 2009; Chang and Snyder, 2010):

$$\text{Firing rate} = a \times \exp^{-\frac{(x-\mu)^2}{2\sigma^2}} \times (1 + g_H H + g_G G) + b,$$

where

$$x = T - (wG + (1 - w)H).$$

In this model, target position is constrained to be coded with respect to the hand ( $w = 0$ ,  $x = T-H$ ) or the gaze ( $w = 1$ ,  $x = T-G$ ), or to have a frame of reference dependent on both hand position and gaze position (values of  $w$  other than 0 or 1). Gain fields for hand and gaze position were accounted for separately in the model by the parameters  $g_H$  and  $g_G$  (see **Experimental Procedures** for more details about the model).

The cell shown in **Figure 3** was well fit by the model ( $r^2 = 0.87$ ) and had a weight parameter,  $w$ , of 0.03, which corresponds to a hand-centered reference frame and is consistent with the results from the separability analysis. A six-parameter hand-centered model with  $x = T-H$  fit the firing rates for this cell just as well as the full seven-parameter model (F test,  $p = 0.43$ ;  $r^2 = 0.87$ ), whereas models with  $x = T-G$  (gaze-centered) and  $x = T$  (body- or screen-centered) fit the data significantly worse than the full model ( $r^2 = 0.47$  and  $r^2 = 0.54$  respectively,  $p < 0.00001$  for both F tests).

**Figure 6** shows the distribution of the weight parameter  $w$  across the population of recorded cells ( $n = 128$ ). The median value was 0.04, and the modal bin was the one centered on  $w = 0$  (hand centered). Consistent with other recent reports (McGuire and Sabes, 2011), the population was not homogeneous and contained some gaze-centered cells ( $w \sim 1$ ) as well as cells with an intermediate reference frame ( $0 < w < 1$ ). However, the overall trend in the population was toward

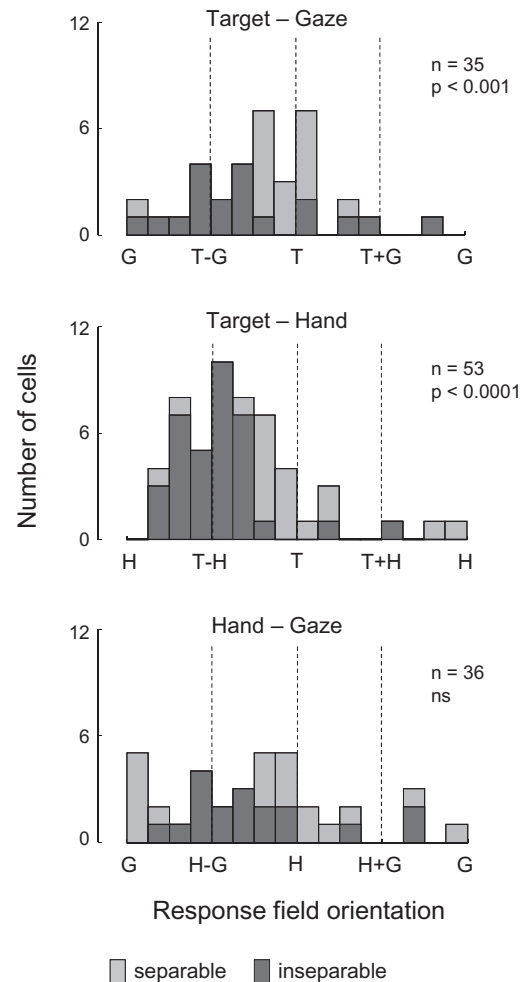


**Figure 4. Area 5d Predominantly Codes the Reach Vector: Target-Hand**

Histograms show the response field orientations for the population of tuned cells for each pair of variables. Stacked bars represent inseparable (dark gray) or separable (light gray) responses. p values reflect the result of the Kuiper test for uniformity. The dominance of T-H coding is also present away from the response field peak.

See **Figure S2**.

a hand-centered representation, supporting the results from the SVD/gradient analysis. The hand-centered model fit as well as the full model in 38% of cells (F test,  $p > 0.01$ ), whereas the gaze-centered model fit as well as the full model in only 17% of cells. The full model fit better than either reduced model in 29% of cells and both reduced models fit as well as the full model in the remaining 16% of cells.

The model uses a Gaussian function for fitting, which is appropriate for cells with a peaked response. Most of our recorded cells (108/128; 84%) had a response peak within the working range. The shape of the weights distribution when including only these cells was very similar to that for the entire population (**Figure S3A**), as was the distribution for the subset of cells with values of  $r^2$  greater than 0.6 ( $n = 75$ ; **Figure S3B**).

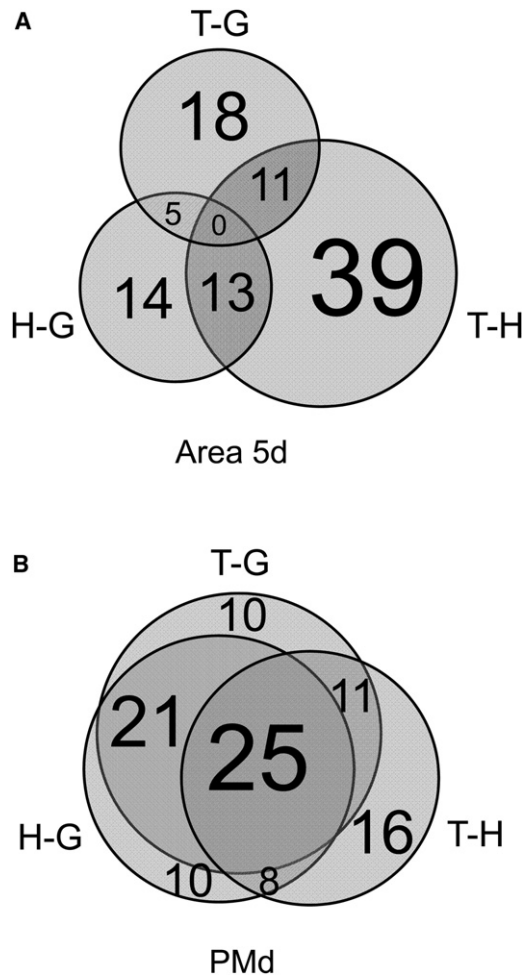


**Figure 5. Coding in Area 5d is Distinct from that in the Dorsal Premotor Cortex**

The percentage of tuned, inseparable cells that code each vector in (A) area 5d and (B) dorsal premotor cortex. (Data in Figure 5B taken from Pesaran et al., 2010.)

## DISCUSSION

We found that the reach vector, or target position relative to the hand, is the principal representation in parietal area 5d during planning of reaches, and that there is a marked absence of coding for the position of the hand relative to gaze (Figures 4, 5, and 6). This hand-centered coding is distinct from the predominantly gaze-centered reference frame reported for the neighboring PRR (Batista et al., 1999; Buneo et al., 2002; Pesaran et al., 2006) and suggests that the two regions subserve different functions. There is evidence that the reach plan is transformed from gaze coordinates to hand coordinates in PRR, possibly by a gain field of the distance between the hand and the gaze (Chang et al., 2009). It appears that this transformation has been largely completed prior to area 5d, suggesting that area 5d is downstream of other, more cognitive, nodes of the reaching network. This suggestion is consistent with findings

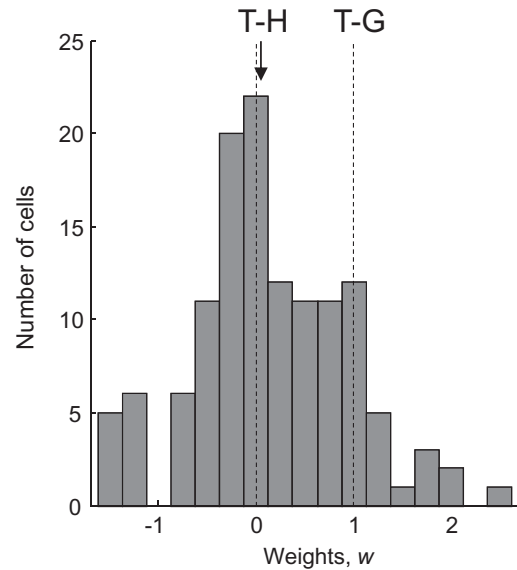


**Figure 6. Distribution of Weights in the Parametric Modeling Analysis**

The arrowhead indicates the median weight value (0.04). The distribution is similar for cells with a peak in the working range and cells with  $r^2$  greater than 0.6.

See Figure S3.

showing that area 5d is involved in motor preparation (Maimon and Assad, 2006) and codes only selected reaches rather than potential reach plans (Cui and Andersen, 2011).

Delays in visual and proprioceptive feedback during movement are sufficiently long that instability and errors quickly occur if the motor control system relies solely on sensory feedback. Instead, it is thought that the brain generates estimates of the current and future states of the arm by combining a copy of the command signal produced by motor cortex with a model of the dynamics of the limb (Desmurget and Grafton, 2000; Wolpert and Miall, 1996). Posterior parietal cortex, and area 5 in particular, is a good candidate for state estimation of the arm because it receives efference copy signals as well as visual and proprioceptive inputs and has been shown to contain neurons that best reflect forward movement states (Archambault et al., 2009; Mulliken et al., 2008). The task used in our study is static and cannot speak directly to whether area 5d is the locus for a forward model, but the strong bias toward coding of the upcoming reach vector, as opposed to a more gaze-centered signal, is consistent with this hypothesis.

There has been recent debate about the existence and functional necessity of distinct reference frames in different subregions of the brain. Large numbers of cells with mixed or intermediate reference frames have been described in parietal (Avillac et al., 2005; Chang and Snyder, 2010; McGuire and Sabes, 2011; Mulette-Gillman et al., 2005, 2009; Stricanne et al., 1996) and frontal (Batista et al., 2007) regions, with the frequent interpretation that an orderly progression of coordinate transformations does not exist. However, it is likely that the discrepancies between these reports and our findings are due

to differences in experimental design and interpretation of the data. Of the studies involving reaches, several did not use enough conditions to be able to distinguish clearly whether changes in firing rate were due to reference frame shifts or to postural gain fields (Batista et al., 2007; McGuire and Sabes, 2011), a distinction that is critical for determining the appropriate reference frame. The combination of a full matrix of variables and the gradient analysis and SVD of the response matrices used in this study was specifically devised to minimize such difficulties.

Several of the studies quantified the reference frame by fitting the data to a nonlinear parametric model, as we also did in addition to our main analysis (see Figure 6). This approach has some distinct advantages: for cells with a good fit to the model, this framework allows testing of very specific hypotheses relating to the parameters being fit, such as where the reference frame lies on a continuum between hand centered and gaze centered. In our case, it also allowed us to use the entire data set for each cell rather than looking only at the peak of the tuning curves, as is the case in the matrix analysis (although see also Figure S2). However, it has the disadvantage that the data are forced into a prespecified model, which may not be appropriate. For example, the relative coding of hand, gaze, and target position observed in dorsal premotor cortex and revealed through SVD and gradient analyses (Pesaran et al., 2006) would most likely have appeared intermediate and difficult to interpret if analyzed through a modeling framework restricted to combinations of gaze and hand-centered tuning only.

In agreement with recent results from other groups, we did observe some heterogeneity at the single-cell level in area 5d and relatively few “purely” hand-centered cells. Although the results of the modeling analysis show a clear peak at weight values associated with a hand-centered reference frame, there are also cells with intermediate and gaze-centered reference frames (Figure 6). Conversely, others have observed a consistent bias toward gaze-centered coding in PRR (Chang and Snyder, 2010) and hand-centered coding in area 5d (McGuire and Sabes, 2011) but chose to focus on the population of intermediate cells. Hence, much of the data are consistent across groups despite differences in interpretation.

A longstanding model of sensorimotor integration postulates a common, gaze-centered, reference frame gain modulated by eye, head, and limb postural signals to enable read-out in multiple reference frames (Andersen et al., 1998). Advantages of this include a reduction in the number of sequential transformations necessary (for example, from gaze to limb directly, rather than gaze to head to body to limb), parsimonious incorporation of error signals generated from visual feedback, and computational benefits from using the same reference frame for reaches as for saccades. A more recent approach casts parietal neurons as jointly encoding a set of basis functions with no single underlying reference frame but instead many different combinations of intermediate reference frames (Pouget and Snyder, 2000). The number of cells required for the basis set would increase exponentially with the number of different signals to be integrated. Taken to its extreme, this theory would predict that the signals involved in sensorimotor transformations would be extremely distributed across a large,

heterogeneous area and systematic reference frames from region to region would not be observed. This theory is not consistent with what we report here for area 5d or what has previously been reported for PRR. However, a reduced version of the basis function theory with a limited number of inputs (for example, retinotopic target location and nonlinear postural gain signals) is compatible with the data and, indeed, would be equivalent to earlier models.

Intermediate representations were initially reported by our lab in the lateral intraparietal area (LIP) of the posterior parietal cortex (Stricanne et al., 1996). Gain modulation models show intermediate representations when there are multiple input and output representations to the hidden layer of a 3-layer neural network performing coordinate transformations (Xing and Andersen, 2000). However, the data from this study and those of Pesaran et al. (2006, 2010) establish that there are distinct, modular reference frames in different cortical areas, as well as gain fields and intermediate representations, and this puts some constraints on the types of computational models that are neurobiologically relevant. The intermediate representations and gain fields may be a part of the transformation process (Xing and Andersen, 2000; Zipser and Andersen, 1988). The presence of distinct representations is shown by the more complete analysis of response field variables and the different patterns of spatial representation between areas reported in the current study for area 5d and previous studies of PRR and PMd (Pesaran et al., 2006, 2010). Moreover, it is likely that future findings will reveal an even greater degree of differentiation of spatial representations based on better circuit analysis and understanding. For instance, different layers or cell types may show different reference frame representations, gain fields, or intermediate representations and may account for the apparent heterogeneity seen when sampling from an entire cortical area.

We argue that our results show that there is a strong representation of the reach vector in area 5d, but we would not claim that this area codes exclusively in hand-centered coordinates and has no other role or representations. We did not test explicitly for a body-centered representation (Lacquaniti et al., 1995), although this would have shown up in our data as peaks in the population histograms at T for target-gaze and target-hand plots (Figure 4). There are many other potential representations, such as shoulder centered, that we did not test for. Moreover, all of the stimuli and movements in our experiment were confined to a two-dimensional frontal plane, and the animals had been trained to maintain fixation during the task, which is unnatural compared with conditions of free gaze. However, one of the strengths of this study is that the experimental design and main analysis closely match that used by Pesaran et al., so we are able compare and contrast the results for the same task in three different parietal and frontal regions (Pesaran et al., 2006, 2010). PRR, area 5d, and PMd all show clearly different population patterns of coding under this analysis, with PRR coding predominantly T-G, area 5d coding predominantly T-H, and PMd coding T-G, T-H, and H-G for both reaches and saccades. This suggests that although they are heavily interconnected, each node has a distinct role in the formation of the plans for action.

## EXPERIMENTAL PROCEDURES

Two adult male rhesus monkeys (*Macaca mulatta*, G and T) participated in this study. All surgical and animal care procedures were conducted in accordance with National Institutes of Health guidelines and were approved by the California Institute of Technology Animal Care and Use Committee.

### Behavioral Tasks

The monkeys were head fixed and trained to reach with the left arm to a touch-sensitive screen (Elo TouchSystems, Menlo Park, CA) placed in front of an LCD monitor. Eye position was monitored with an infrared eye-tracking camera (ISCAN, Arrington Research). Figure 1A illustrates the behavioral paradigm. At the start of each trial, the animal was required to fixate his eyes on a small red square and to touch a small green square. After a 1 s fixation period, a second green square (the target) was illuminated. The monkey continued to hold the ocular and manual fixations for a variable delay period (1.2–1.5 s) until the initial manual fixation point was extinguished. This was the signal for the animal to reach to the target location while maintaining visual fixation. If the animal successfully acquired the target within 0.7 s and then held his hand on it for 0.25 s without moving his gaze, he was rewarded with a drop of juice. Behavioral tolerance windows had radii of 4 degrees (eye fixation) and 5 degrees (initial hand position and target).

In the center-out task, the initial ocular and manual fixation points were next to each other in the center of the screen and eight reach targets were spaced evenly around the fixation points at 20 degree eccentricity. In this task, the target was extinguished after 0.4 s and the animal made a reach to a remembered location 0.8–1.1 s later. In the reference frame task (Figure 1B), the initial hand position (H) was at  $-20$ ,  $-10$ ,  $0$ , or  $10$  degrees along a horizontal line (screen-centered coordinates) and the gaze fixation positions (G) varied across the same four positions. The reach target (T) was also at one of four locations ( $-20$ ,  $-10$ ,  $0$ , or  $10$  degrees) on a horizontal line either 16 degrees above or below the fixation positions, whichever would best activate the cell. The 4 gaze fixations, 4 hand fixations, and 4 target positions combined to give a total of 64 different trial types. In this task, the target remained illuminated throughout the delay period to make the task easier for the monkeys to perform. Previous studies of area 5d show that cells here have little or no direct response to the onset of the visual cue (Cui and Andersen, 2011), so it is unlikely that recorded neural activity during the delay period is due to the ongoing visual stimulation. All reaches were made within the frontal plane formed by the touchscreen, which was at a distance of 30 cm (monkey G) or 26 cm (monkey T) from the eyes.

### Data Collection

In both animals, a recording chamber was implanted over the right posterior parietal cortex under isoflurane anesthesia. Structural magnetic resonance imaging was used to verify the placement of each chamber above Brodmann area 5 and to guide the location of recording sites. Single-unit recordings were made with  $\sim 1$ – $2$  M $\Omega$  Pt/Ir microelectrodes in a single-channel microdrive (FHC, Boudoin, ME) from dorsal area 5 (area 5d) in the surface cortex adjacent to the medial bank of the intraparietal sulcus (IPS) (Figure 1C). Recordings spanned approximately 3 mm rostral to the IPS and were between 0.14 and 3.5 mm in depth from the estimated cortical surface, with a median depth of 0.93 mm.

Recorded neural activity was passed through a headstage (Omnetics), then filtered (154–8.8 KHz), amplified, and digitized (Plexon, Dallas, TX) and saved for offline sorting (Plexon Offline Sorter) and analysis (Matlab 7.8, Mathworks, Natick, MA). Cells were first isolated and then recorded during the center-out task. If a cell showed a tuned response to reach location in this task (assessed by one-way ANOVA,  $p < 0.01$ ) and continued to be stable, the experiment then moved on to the main reference frame task. In some sessions, additional well-isolated neurons were recorded on the same electrode: these were included in the analysis regardless of tuning.

### Data Analysis

Only well-isolated single units with a minimum of three trials per condition were analyzed. Unless otherwise specified, trials were aligned at movement

onset (0 ms). The delay epoch was defined as the period from  $-500$  ms to  $-100$  ms (see Figure 3).

Gradient analysis (Buneo et al., 2002) was used to determine which variable within a pair (TH, TG, or HG) exerted the most influence on the firing rate of a cell or whether both had equivalent influence. The gradient of the response matrix was estimated with the Matlab gradient function. The angle for each element was doubled to account for symmetrical response fields before computing the resultant. The response field was classed as tuned if the resultant length was significantly greater than the resultant length calculated after randomization of the matrix elements (randomization test). The angle of the resultant indicated the orientation of the response field and the relative influence of each variable on the firing rate.

SVD analysis (Peña and Konishi, 2001; Pesaran et al., 2006, 2010) was used to assess whether the relationship between pairs of variables was separable (in other words, a multiplicative, gain relationship) or inseparable. For a response matrix of hand position (H) and target position (T) (with gaze [G] held constant), SVD reduces the matrix to a weighted sum where the weights ( $s_1$ ,  $s_2$ , etc.) are known as the singular values:

$$f(T, H) = s_1 t_1(T) h_1(H) + s_2 t_2(T) h_2(H) + \dots$$

If the first singular value is very large such that the second and further terms are insignificant, then the matrix can be adequately described by the first term alone:  $f(T, H) = s_1 t_1(T) h_1(H)$ . In this case, changes in H and T produce multiplicatively separable changes in the response of the cell, which is the definition of gain field coding. If two or more singular values are necessary to capture the response matrix, then H and T are inseparable and their relationship cannot be modeled as a gain effect of one variable on the other. Matrices were mean subtracted before performing the SVD. A matrix was classified as separable if the first singular value was significantly large ( $p < 0.05$ ) when compared with the first singular value obtained after randomization of the matrix elements. Otherwise, the matrix was deemed inseparable. It has been shown previously that this method is sufficiently sensitive to detect gain fields with as few as three trials per condition (Pesaran et al., 2010).

It is important to note that the gradient analysis and SVD were used in conjunction with one another rather than separately. The gradient analysis indicates the extent to which the firing rate of the cell depends on changes in H or T; however, for cells in which both H and T influence the firing rate, this analysis cannot distinguish between gain field and vector encoding (see Figures 2B and 2D), and the SVD is used to provide this information. Similarly, SVD was performed only on matrices that showed significant tuning in the gradient analysis. This allowed the categorization of a matrix as inseparable to be more meaningful than it would be if SVD was performed on all cells, including those which were not tuned to either variable.

To test whether individual cells coded exclusively for the target relative to the hand (T-H), we scored each cell on three criteria for each of the three variable-pair matrices (nine criteria in total): (1) does the matrix show significant tuning; (2) is the response field appropriately oriented ( $-90$  degrees for the TH matrix,  $0$  degrees for the TG and HG matrices; see Table 1; tolerance  $\pm 60$  degrees); and (3) does the response field have the appropriate SVD categorization (inseparable for the TH matrix, separable for the TG and HG matrices; see Table 1)? If a cell scored at least 8/9 according to these criteria, then it was classed as coding purely in hand-centered coordinates. A similar classification was conducted for target-gaze and hand-gaze encoding (see Table 1 for the appropriate response field orientations and SVD categorizations).

### Modeling

For each cell, we fit the delay-period firing rates from all 64 trial types to a parametric model based on a Gaussian tuning curve, similarly to the model used by Chang et al. (2009):

$$\text{Firing rate} = a \times \exp^{-\frac{(x-\mu)^2}{2\sigma^2}} \times (1 + g_H H + g_G G) + b,$$

where

$$x = T - (wG + (1 - w)H).$$

The inputs to the model were the mean delay-period firing rates (spk/s) in the 64 different conditions and the corresponding positions of the hand (H), gaze (G), and target (T) in screen-centered degrees of visual angle (degrees). The parameters fit were peak amplitude ( $a$ , constrained to  $-300$  to  $300$  spk/s), the offset from center ( $\mu$ , constrained to  $-50$  to  $50$  degrees) and standard deviation ( $\sigma$ , constrained to  $3$  to  $60$  degrees) of the Gaussian tuning curve, the amplitude of the hand ( $g_H$ ) and gaze ( $g_G$ ) gain fields (both constrained to  $-0.4$  to  $0.4$  modulation/degrees), baseline firing ( $b$ , constrained to  $-5$  to  $100$  spk/s), and the weight parameter ( $w$ , unitless, constrained to  $-1.5$  to  $2.5$ ).

#### SUPPLEMENTAL INFORMATION

Supplemental Information includes three figures and can be found with this article online at <http://dx.doi.org/10.1016/j.neuron.2012.03.041>.

#### ACKNOWLEDGMENTS

This work was supported by National Institutes of Health Grant EY005522. We thank Tessa Yao for editorial assistance, Kelsie Pejsa and Nicole Sammons for animal care, Igor Kagan for magnetic resonance imaging, Viktor Shcherbatyuk for technical assistance, and Bijan Pesaran and Matthew Nelson for helpful discussions.

Accepted: May 21, 2012

Published: July 25, 2012

#### REFERENCES

- Andersen, R.A., and Mountcastle, V.B. (1983). The influence of the angle of gaze upon the excitability of the light-sensitive neurons of the posterior parietal cortex. *J. Neurosci.* **3**, 532–548.
- Andersen, R.A., and Buneo, C.A. (2002). Intentional maps in posterior parietal cortex. *Annu. Rev. Neurosci.* **25**, 189–220.
- Andersen, R.A., and Cui, H. (2009). Intention, action planning, and decision making in parietal-frontal circuits. *Neuron* **63**, 568–583.
- Andersen, R.A., Essick, G.K., and Siegel, R.M. (1985). Encoding of spatial location by posterior parietal neurons. *Science* **230**, 456–458.
- Andersen, R.A., Bracewell, R.M., Barash, S., Gnadt, J.W., and Fogassi, L. (1990). Eye position effects on visual, memory, and saccade-related activity in areas LIP and 7a of macaque. *J. Neurosci.* **10**, 1176–1196.
- Andersen, R.A., Snyder, L.H., Batista, A.P., Buneo, C.A., and Cohen, Y.E. (1998). Posterior parietal areas specialized for eye movements (LIP) and reach (PRR) using a common coordinate frame. *Novartis Foundation Symposium* **218**, 109–122, discussion 122–128, 171–175.
- Archambault, P.S., Caminiti, R., and Battaglia-Mayer, A. (2009). Cortical mechanisms for online control of hand movement trajectory: the role of the posterior parietal cortex. *Cereb. Cortex* **19**, 2848–2864.
- Avillac, M., Deneve, S., Olivier, E., Pouget, A., and Duhamel, J.R. (2005). Reference frames for representing visual and tactile locations in parietal cortex. *Nat. Neurosci.* **8**, 941–949.
- Batista, A.P., Buneo, C.A., Snyder, L.H., and Andersen, R.A. (1999). Reach plans in eye-centered coordinates. *Science* **285**, 257–260.
- Batista, A.P., Santhanam, G., Yu, B.M., Ryu, S.I., Afshar, A., and Shenoy, K.V. (2007). Reference frames for reach planning in macaque dorsal premotor cortex. *J. Neurophysiol.* **98**, 966–983.
- Battaglia-Mayer, A., Caminiti, R., Lacquaniti, F., and Zago, M. (2003). Multiple levels of representation of reaching in the parieto-frontal network. *Cereb. Cortex* **13**, 1009–1022.
- Blohm, G., Keith, G.P., and Crawford, J.D. (2009). Decoding the cortical transformations for visually guided reaching in 3D space. *Cereb. Cortex* **19**, 1372–1393.
- Bremmer, F., Graf, W., Ben Hamed, S., and Duhamel, J.R. (1999). Eye position encoding in the macaque ventral intraparietal area (VIP). *Neuroreport* **10**, 873–878.
- Buneo, C.A., Jarvis, M.R., Batista, A.P., and Andersen, R.A. (2002). Direct visuomotor transformations for reaching. *Nature* **416**, 632–636.
- Caminiti, R., Ferraina, S., and Mayer, A.B. (1998). Visuomotor transformations: early cortical mechanisms of reaching. *Curr. Opin. Neurobiol.* **8**, 753–761.
- Chang, S.W., and Snyder, L.H. (2010). Idiosyncratic and systematic aspects of spatial representations in the macaque parietal cortex. *Proc. Natl. Acad. Sci. USA* **107**, 7951–7956.
- Chang, S.W., Papadimitriou, C., and Snyder, L.H. (2009). Using a compound gain field to compute a reach plan. *Neuron* **64**, 744–755.
- Cohen, Y.E., and Andersen, R.A. (2000). Reaches to sounds encoded in an eye-centered reference frame. *Neuron* **27**, 647–652.
- Cohen, Y.E., and Andersen, R.A. (2002). A common reference frame for movement plans in the posterior parietal cortex. *Nat. Rev. Neurosci.* **3**, 553–562.
- Cui, H., and Andersen, R.A. (2011). Different representations of potential and selected motor plans by distinct parietal areas. *J. Neurosci.* **31**, 18130–18136.
- Desmurget, M., and Grafton, S. (2000). Forward modeling allows feedback control for fast reaching movements. *Trends Cogn. Sci.* **4**, 423–431.
- Flanders, M., Helms-Tillery, S.I., and Soechting, J.F. (1992). Early stages in a sensorimotor transformation. *Behav. Brain Sci.* **15**, 309–362.
- Galletti, C., Battaglini, P.P., and Fattori, P. (1995). Eye position influence on the parieto-occipital area PO (V6) of the macaque monkey. *Eur. J. Neurosci.* **7**, 2486–2501.
- Kalaska, J.F., Scott, S.H., Cisek, P., and Sergio, L.E. (1997). Cortical control of reaching movements. *Curr. Opin. Neurobiol.* **7**, 849–859.
- Lacquaniti, F., Guigon, E., Bianchi, L., Ferraina, S., and Caminiti, R. (1995). Representing spatial information for limb movement: role of area 5 in the monkey. *Cereb. Cortex* **5**, 391–409.
- Maimon, G., and Assad, J.A. (2006). Parietal area 5 and the initiation of self-timed movements versus simple reactions. *J. Neurosci.* **26**, 2487–2498.
- McGuire, L.M., and Sabes, P.N. (2009). Sensory transformations and the use of multiple reference frames for reach planning. *Nat. Neurosci.* **12**, 1056–1061.
- McGuire, L.M., and Sabes, P.N. (2011). Heterogeneous representations in the superior parietal lobule are common across reaches to visual and proprioceptive targets. *J. Neurosci.* **31**, 6661–6673.
- Mullette-Gillman, O.A., Cohen, Y.E., and Groh, J.M. (2005). Eye-centered, head-centered, and complex coding of visual and auditory targets in the intraparietal sulcus. *J. Neurophysiol.* **94**, 2331–2352.
- Mullette-Gillman, O.A., Cohen, Y.E., and Groh, J.M. (2009). Motor-related signals in the intraparietal cortex encode locations in a hybrid, rather than eye-centered reference frame. *Cereb. Cortex* **19**, 1761–1775.
- Mulliken, G.H., Musallam, S., and Andersen, R.A. (2008). Forward estimation of movement state in posterior parietal cortex. *Proc. Natl. Acad. Sci. USA* **105**, 8170–8177.
- Nakamura, K., Chung, H.H., Graziano, M.S., and Gross, C.G. (1999). Dynamic representation of eye position in the parieto-occipital sulcus. *J. Neurophysiol.* **81**, 2374–2385.
- Peña, J.L., and Konishi, M. (2001). Auditory spatial receptive fields created by multiplication. *Science* **292**, 249–252.
- Pesaran, B., Nelson, M.J., and Andersen, R.A. (2006). Dorsal premotor neurons encode the relative position of the hand, eye, and goal during reach planning. *Neuron* **51**, 125–134.
- Pesaran, B., Nelson, M.J., and Andersen, R.A. (2010). A relative position code for saccades in dorsal premotor cortex. *J. Neurosci.* **30**, 6527–6537.
- Pouget, A., and Snyder, L.H. (2000). Computational approaches to sensorimotor transformations. *Nat. Neurosci. Suppl.* **3**, 1192–1198.
- Pouget, A., Deneve, S., and Duhamel, J.R. (2002). A computational perspective on the neural basis of multisensory spatial representations. *Nat. Rev. Neurosci.* **3**, 741–747.

Stricanne, B., Andersen, R.A., and Mazzoni, P. (1996). Eye-centered, head-centered, and intermediate coding of remembered sound locations in area LIP. *J. Neurophysiol.* *76*, 2071–2076.

Wolpert, D.M., and Miall, R.C. (1996). Forward Models for Physiological Motor Control. *Neural Netw.* *9*, 1265–1279.

Xing, J., and Andersen, R.A. (2000). Models of the posterior parietal cortex which perform multimodal integration and represent space in several coordinate frames. *J. Cogn. Neurosci.* *12*, 601–614.

Zipser, D., and Andersen, R.A. (1988). A back-propagation programmed network that simulates response properties of a subset of posterior parietal neurons. *Nature* *331*, 679–684.